Chemical Physics Letters 594 (2014) 34–40

Contents lists available at ScienceDirect

Chemical Physics Letters

journal homepage: www.elsevier.com/locate/cplett

Solid-state NMR investigation of the $^{16/17}O$ isotope exchange of oxygen species in pure-anatase and mixed-phase TiO_2

Xiaoming Sun [a,b], Michael Dyballa [b], Junqing Yan [a], Landong Li [a,*], Naijia Guan [a], Michael Hunger [b,*]

[a] Key Laboratory of Advanced Energy Materials Chemistry (Ministry of Education), College of Chemistry, Nankai University, Tianjin 300071, PR China
[b] Institute of Chemical Technology, University of Stuttgart, 70550 Stuttgart, Germany

ARTICLE INFO

Article history:
Received 25 November 2013
In final form 9 January 2014
Available online 15 January 2014

ABSTRACT

Quantitative ^{17}O MAS NMR investigation of the $^{16/17}O$ isotope exchange on pure-anatase TiO_2/A and mixed-phase TiO_2/A + R with an anatase to rutile ratio of 1:1 has been performed. Evaluation of the exchange kinetics hints to a strong decrease of the activation energy of this reaction on mixed-phase TiO_2/A + R material (61 (A) and 70 kJ/mol (R)) compared with pure-anatase TiO_2/A (105 kJ/mol). Furthermore, a very rapid increase of the ^{17}O MAS NMR signals of surface oxygen species indicates a preferred $^{16/17}O$ isotope exchange at these sites and a subsequently exchange with ^{16}O framework atoms in the anatase and rutile domains.

1. Introduction

Heterogeneous photocatalysis has been attracting researchers' attention since the water splitting on photoexcited TiO_2 was discovered by Fujishima and Honda in 1972 [1], due to its potential for applications in solar energy conversion. TiO_2 is still one of the most extensively studied materials because of its superior photocatalytic activity, high resistance to photocorrosion, and nontoxicity [2]. Furthermore, TiO_2 is widely employed as conventional catalyst support [3], pigment [4], photocatalysts [5,6], and components of solar cells [7,8]. As often described, the two common phases, which are applied for photocatalysis, are anatase and rutile. The rutile phase is the most stable structure of TiO_2, while the anatase phase can transform to rutile at high temperatures [9]. Both anatase and rutile consist of TiO_6 groups, which are joined together by sharing different numbers of edges – two in rutile and four in anatase. The single oxygen site in each phase is trigonally coordinated (OTi_3) with average bond lengths of 0.1959 nm for rutile and 0.1946 nm for anatase [10]. Zhang et al. [11,12] studied the phase transition from anatase to rutile by Raman spectroscopy and X-ray diffraction and found that the photocatalytic activity of TiO_2 is related to specific surface species. They observed that phase junctions formed between the anatase and rutile domains enhance the hydrogen production in the photocatalytic water splitting.

Generally, the study of the oxygen isotope exchange is an effective way for understanding the reactivity of oxygen species on oxide surfaces. A number of oxygen isotope exchange (OIE) investigations performed by Boreskov, Winter, Novakova, and others have been performed by using ^{18}O-enriched oxygen gas and mass spectroscopy of the gas phase to obtain insights into the mechanisms of OIE on various oxides [13–15]. Generally, an exchange of the surface oxygen atoms $^{16}O_s$ on solid oxides with ^{18}O atoms of $^{18}O_2(g)$ gas occurs via the reactions R_1 and R_2 in Eqs.(1) and (2), respectively [13–15]:

$$^{18}O_2(g) + {}^{16}O_s \rightarrow {}^{18}O{}^{16}O(g) + {}^{18}O_s \quad (1)$$

$$^{18}O_2(g) + 2{}^{16}O_s \rightarrow {}^{16}O_2(g) + 2{}^{18}O_s \quad (2)$$

This OIE can be induced by thermal treatment [13–15,16] or UV/Vis irradiation [17,18]. The same is valid for an exchange of oxygen in solid oxides with $^{17}O_2$ gas. By measuring the OIE via mass spectrometry, the activation energy for this reaction on V_2O_5, Cr_2O_3, MnO_2, Fe_2O_3, Co_3O_4, NiO, CuO, and ZnO vary from E_a = 103 to 258 kJ/mol in the case of an R^1 mechanism and from E_a = 83 to 211 kJ/mol for the R^2 mechanism [16]. Winter and Sturge [14] found that the oxygen isotope exchange reactions on pure-anatase and pure-rutile TiO_2 occurs via the R^1 mechanism with activation energies of E_a = 134 and 144 kJ/mol, respectively. Pichat et al. [18] considered the lability of surface oxygen atoms as a reason of the UV/Vis-induced oxygen isotope exchange properties of TiO_2 [18]. Sato et al. [17] could show that the oxygen isotope exchange capacity of TiO_2, induced by UV/Vis irradiation, correlates well with the activity in the photocatalytic oxidation of ethane.

^{17}O solid-state nuclear magnetic resonance (SSNMR) spectroscopy with rapid spinning of the powder samples around an axis

* Corresponding authors. Fax: +86 22 2350 0341 (L. Li), +49 711 685 64081 (M. Hunger).
E-mail addresses: lild@nankai.edu.cn (L. Li), michael.hunger@itc.uni-stuttgart.de (M. Hunger).

http://dx.doi.org/10.1016/j.cplett.2014.01.014
0009-2614/

in the magic angle (MAS: magic angle spinning) to the direction of the magnetic field B_0 is a powerful method for investigating and distinguishing the various local structures of oxygen atoms in TiO_2 materials [19–22]. As a specific property, ^{17}O nuclei have the nuclear spin $I = 5/2$ and are, therefore, quadrupole nuclei. In this case, the position and shape of their ^{17}O MAS NMR signals are strongly affected by the quadruploar interaction of the electric quadrupole moment (eQ) of the ^{17}O nuclei and the electric field gradient ($V_{zz} = eq$) at the position of the resonating nuclei. The most important SSNMR parameters describing quadrupolar interactions are the quadrupole coupling constant $C_q = e^2qQ/h$ (h: Planck constant) and the asymmetry parameter $\eta_q = (V_{yy} - V_{xx})/V_{zz}$, which depends on the principal axes values of the electric field gradient V_{ii} (ii = xx, yy, zz) [23,24].

The present work focuses on the study of the $^{16/17}O$ isotope exchange on pure anatase in comparison with a mixed-phase TiO_2 material containing anatase and rutile domains as well as various surface oxygen species and phase conjunctions on the anatase and rutile domains. ^1H and ^{17}O MAS NMR spectroscopy were utilized for studying the type as well as density of surface TiOH groups and the ^{17}O atoms in TiO_2 materials, respectively, upon a thermally induced $^{16/17}O$ isotope exchange with $^{17}O_2$ gas. Furthermore, the activation energies of the OIE were determined. To the best of our knowledge, this is the first quantitative ^{17}O solid-state NMR investigation of the $^{16/17}O$ isotope exchange of oxygen species on pure and mixed-phase TiO_2 materials.

2. Experimental section

2.1. Preparation of the TiO_2 materials

All chemicals used for the TiO_2 synthesis were of analytical grade, purchased from Alfa Aesar Chemical Co., and used as received without further purification. The TiO_2 materials were prepared via an ionic liquid (IL) assisted hydrothermal method according to a modified procedure described in literature [25].

For the synthesis of the ^{17}O-enriched reference material consisting of pure anatase (TiO_2/Reference), 10 g of ^{17}O-enriched H_2O (^{17}O-enrichment of 20%, Cambridge Isotope Lab., Inc., USA) and 1 ml of 48% aqueous solution of H_2SO_4 were added successively to 92 g of 1-butyl-3-methylimidazolium chloride ($bmim^+Cl^-$) in a 250 ml Teflon liner inside an ice-water bath. H_2SO_4 was used for inhibiting the anatase to undergo phase transformation to rutile [26]. This mixture was stirred until a clear yellow liquid was formed. Then, 50 g of $TiCl_4$ was slowly added. During the mixing process, HCl gas was released as a product of the hydrolysis of $TiCl_4$ with the water in the solution. At the same time, a yellow solid was formed gradually in the mixture, which was purged by dry N_2 gas to remove the HCl gas. Afterwards, the Teflon liner was put into a stainless steel autoclave heated at 140 °C for 1 h. During this time, the yellow solid became melted and stirred to be homogenous and fully converted. Finally, the mixture was maintained at 150 °C for 2 days for crystallization. After cooling down to room temperature, the product was washed five times by centrifugation and redispersion in ethanol, followed by drying in air at 80 °C for 24 h. The obtained TiO_2/Reference material has a molar ^{17}O-content of 17.8% corresponding to 2.22 mmol/g.

For the synthesis of the non-enriched pure-anatase material (TiO_2/A), the procedure was the same as described before, but distilled conventional water was used instead of ^{17}O-enriched water. The obtained material was calcined at 400 °C for 4 h to remove all organic compounds.

The mixed-phase TiO_2/A + R material was obtained by calcination of the non-enriched TiO_2/A material at 750 °C for 6 h in synthetic air. The phase composition was determined via X-ray diffraction according to $R = I_R/(I_R + 0.8 \cdot I_A)$, in which R is the weight fraction of rutile and I_A and I_R are the peak intensities of the anatase (101) and rutile (110) reflections, respectively [27].

2.2. Characterization methods

X-ray diffraction (XRD) patterns of the calcined samples were recorded on a Bruker D8 diffractometer with CuKα radiation. Transmission electron microscopy (TEM) images of the samples were acquired on a Philips Tecnai G2 20 S-TWIN electron microscope. The specific surface areas of the samples were determined via N_2 adsorption/desorption isotherms collected on a Quantachrome iQ-MP gas adsorption analyzer.

Solid-state NMR investigations were performed on a Bruker Avance III 400WB spectrometer at resonance frequencies of 54.2 MHz for ^{17}O nuclei and 400.1 MHz for ^1H nuclei. The spectra were recorded upon single pulse excitation of $\pi/6$ and $\pi/2$, with repetition times of 0.5 s and 10 s, and sample spinning rates of 20 kHz and 8 kHz using a 2.5 mm and a 4 mm MAS NMR probe for ^{17}O and ^1H MAS NMR spectroscopy, respectively. Before the ^1H MAS NMR studies, the TiO_2 samples were dehydrated in vacuum at 400 °C for 4 h and subsequently sealed in glass tubes until their use. The dehydrated TiO_2 samples were transferred into 4 mm MAS rotors inside a glove box purged with dry nitrogen gas. The TiOH density on the dehydrated TiO_2 materials was determined by comparing the ^1H MAS NMR intensities with that of an external standard consisting of zeolite Na, H-Y, which was obtained by exchange of 35% of the sodium cations by ammonium ions and calcination at 673 K. The simulation and deconvolution of the ^{17}O MAS NMR spectra was performed utilizing the SOLA module of the Bruker BioSpin software TopSpin 3.0, patch level b.58.

2.3. Oxygen isotope exchange experiments

For a typical $^{16/17}O$ isotope exchange experiment, 20.0 ± 0.2 mg of the TiO_2 materials under study filled into a quartz glass tube were evacuated at 673 K in vacuum (pressure below 10^{-2} Pa) for 4 h to remove physisorbed water. Subsequently, 500 mbar of ^{17}O-enriched oxygen gas with an enrichment degree of 85% (ISOTEC, Miamisburg, USA) were loaded on the dehydrated powder sample inside the quartz glass tube (volume of 1 mL) and, then, sealed. Samples with different $^{16/17}O$-exchange degrees were obtained by thermal treatments of the sealed and ^{17}O-loaded TiO_2 samples at 450, 500 or 550 °C for durations up to 100 h.

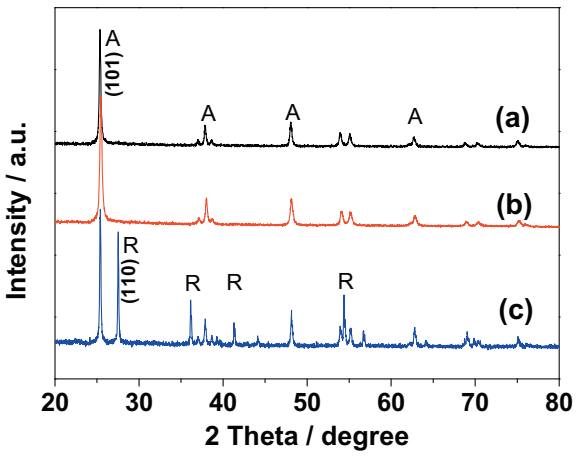

Figure 1. XRD patterns of TiO_2/Reference (a), TiO_2/A (b), and TiO_2/A + R (c).

3. Results and discussion

3.1. Characterization of the catalyst materials

The X-ray patterns of the as-synthesized TiO_2/Reference and TiO_2/A materials in Figure 1a and b reveal the typical diffraction lines of anatase (A). In the X-ray patterns of TiO_2/A + R depicted in Figure 1c, additional reflections of rutile (R) occur, which was formed after calcination at 750 °C. Based on the peak intensities of the anatase (1 0 1) and rutile (1 1 0) reflections, an A:R ratio of 0.53:0.47, i.e. ca. 1:1, was calculated.

The TEM images show that on the one hand the particle size increases from 35 nm to 77 nm (Table 1) upon transformation of pure-anatase TiO_2/A (Figure 2a) to mixed-phase TiO_2 (Figure 2b), respectively. On the other hand, the particle surfaces of the mixed-phase TiO_2 (Figure 2d) are covered by a thick layer of non-ordered material, while the pure-anatase TiO_2 (Figure 2c) shows a very thin surface layer only. The above-mentioned increase of the particle size due to phase transformation agrees with the finding of Yan et al. [28], while the non-ordered surface layers of TiO_2/A + R are very similar to the phase junctions described by Zhang et al. [11,12]. Considering the BET areas of 43 m^2/g for TiO_2/A, the value of 30 m^2/g for mixed-phase TiO_2/A + R can be explained by the growing particle size due to the phase transformation (Table 1). For further characterization of sample TiO_2/Reference, see Supporting information.

3.2. Assignment of the ^{17}O MAS NMR signals of pure-anatase TiO_2/A and mixed-phase TiO_2/A + R

For studying the various types of oxygen species in pure-anatase TiO_2/A and mixed-phase TiO_2/A + R, dehydrated samples of these materials were treated with $^{17}O_2$ gas at 500 °C for 60 h. The ^{17}O MAS NMR spectra of these materials are shown in Figure 3a and b, respectively. In agreement with literature [15], the ^{17}O MAS NMR spectrum of TiO_2/A (Figure 3a) consists of a single signal at 562 ppm with a shape and broadening according to the quadrupole coupling constant of C_q = 1.2 MHz and an asymmetry parameter of η_q = 0.6 (Table 2) corresponding to OTi_3 oxygen species in anatase [19]. In contrast, the spectrum of TiO_2/A + R material contains at least five signals at chemical shifts of 516, 543, 562, 572, and 596 ppm (Figure 3b). Simulation of the spectrum led to the C_q and η_q values summarized in Table 2.

According to Bastow et al. [19], ^{17}O MAS NMR signals at 562 and 596 ppm are caused by OTi_3 species in anatase and rutile domains, respectively. In an earlier ^{17}O MAS NMR study of the commercial mixed-phase TiO_2 photocatalyst P25, signals at 516 and 543 ppm were assigned to distorted OTi_3 and/or tetrahedral oxygen sites (OTi_4) near the surface of anatase [22]. For TiO_2 precursors, Rao et al. [29] observed a ^{17}O MAS NMR signal at 574 ppm assigned to OTi_3 species in low-ordered TiO_2. Therefore, also the signal at 572 ppm observed in the present study is assigned to oxygen species in low-ordered TiO_2 or phase junctions on anatase and rutile domains. In Table 3, the densities of OTi_3 species in anatase (562 ppm) and rutile (596 ppm) domains as well as of surface oxygen species (516, 543, and 572 ppm) in TiO_2/A + R, observed upon $^{16/17}O$ isotope exchange at 550 °C for 60 h are given. These values were determined by comparing the corresponding ^{17}O MAS NMR intensities with that of TiO_2/Reference.

Table 1
Physico-chemical properties of the TiO_2 materials under study.

Sample	Structure	Crystal size[a] (nm)	S_{BET}[b] (m^2g^{-1})
TiO_2/Reference	Anatase	48	27
TiO_2/A	Anatase	35	43
TiO_2/A + R	Anatase + rutile	77	30

[a] Estimated by TEM, accuracy ±10%.
[b] Specific surface area determined by nitrogen adsorption.

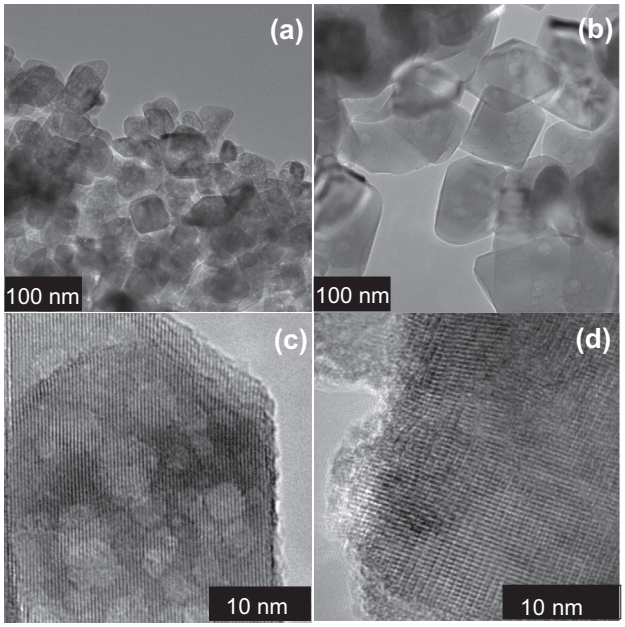

Figure 2. TEM images of TiO_2/A (a and c) and TiO_2/A + R (b and d).

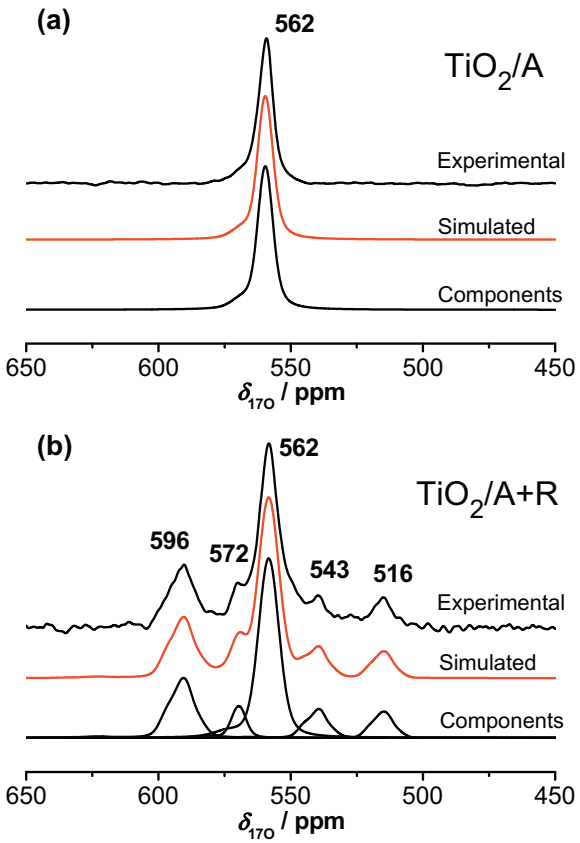

Figure 3. ^{17}O MAS NMR spectra of TiO_2/A (a) and TiO_2/A + R (b) recorded upon $^{16/17}O$ isotope exchange at 500 °C for 60 h.

Table 2
Summary of the ^{17}O MAS NMR signals occurring in the spectra of TiO_2/A and TiO_2/A + R, their chemical shifts δ_{17O}, quadrupole coupling constants C_q, asymmetry parameters η_q, and assignments according to literature (last column).

δ_{17O} (ppm)	C_q (MHz)	η_q	Assignment	References
516	1.8	0.8	Distorted OTi_3 or OTi_4 near the surface	[21]
543	1.6	0.6	Distorted OTi_3 or OTi_4 near the surface	[21,22]
562	1.2	0.6	OTi_3 in anatase	[19]
572	2.0	0.1	OTi_3 in low-ordered TiO_2	[29]
596	1.8	0.6	OTi_3 in rutile	[19]

n.d.: Not determined, because of too low intensity.

Table 3
Densities of TiOH groups and surface oxygen species of different nature (see Table 2) on pure-anatase TiO_2/A (A) and mixed-phase TiO_2/A + R (A + R), determined by quantitative 1H and ^{17}O MAS NMR spectroscopy, respectively, upon $^{16/17}O$ isotope exchange at 500 °C for 60 h.

Surface species	Chemical shift/method	Site density* (mmol/g)
TiOH (A)	1.9 ppm/^{1}H MAS NMR	0.0242
TiOH (A)	6.8 ppm/^{1}H MAS NMR	0.0277
TiOH (A)	11.5 ppm/^{1}H MAS NMR	0.0187
TiOH (A + R)	1.7 ppm/^{1}H MAS NMR	0.0097
TiOH (A + R)	5.1 ppm/^{1}H MAS NMR	0.0497
Surface oxygen (A + R)	516 ppm/^{17}O MAS NMR	0.0069
Surface oxygen (A + R)	543 ppm/^{17}O MAS NMR	0.0207
Surface oxygen (A + R)	572 ppm/^{17}O MAS NMR	0.0109
Oxygen in A (A + R)	562 ppm/^{17}O MAS NMR	0.1330
Oxygen in R (A + R)	596 ppm/^{17}O MAS NMR	0.0380

* Experimental accuracy ±10%.

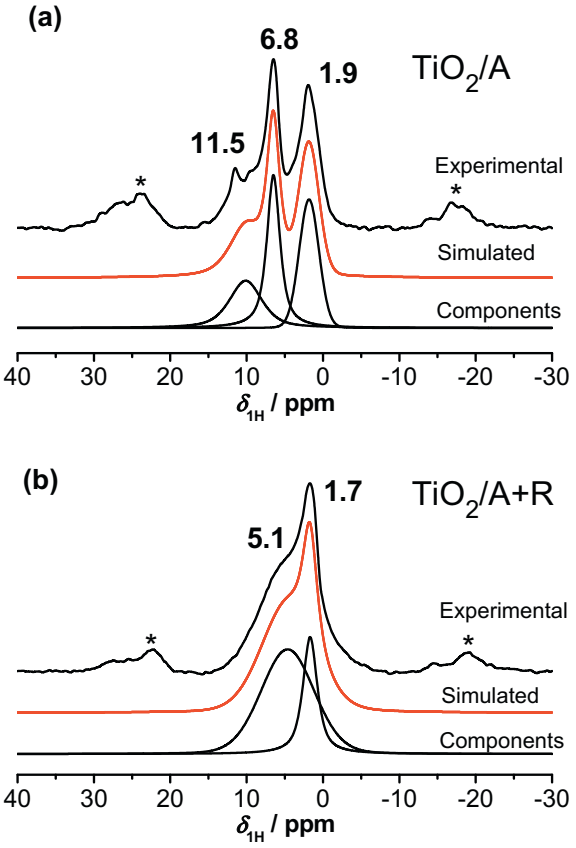

Figure 4. ^{1}H MAS NMR spectra dehydrated TiO_2/A (a) and TiO_2/A + R (b).

3.3. SSNMR investigation of TiOH groups of pure-anatase TiO_2/A and mixed-phase TiO_2/A + R

Studying titanium oxopolymers with static $^1H/^{17}O$ CP NMR spectroscopy (no MAS), a broad ^{17}O solid-state NMR signal extending between −200 and 400 ppm was observed and assigned to oxygen atoms of TiOH groups on TiO_2 [30]. For TiO_2/A and TiO_2/A + R materials investigated in the present work, however, no ^{17}O MAS NMR signal of TiOH groups could be observed in the above-mentioned shift range. Hence, no thermally induced $^{16/17}O$ isotope exchange between ^{16}O atoms of TiOH groups with ^{17}O atoms of the $^{17}O_2$ gas occurred. For characterizing TiOH groups on dehydrated TiO_2/A and TiO_2/A + R materials, therefore, ^{1}H MAS NMR spectroscopy was utilized.

The spectrum of dehydrated TiO_2/A in Figure 4a consists of three well-resolved signals of TiOH groups at 1.9, 6.8, and 11.5 ppm, which agrees well with the observation of Mastkhin et al. [31]. As for many other oxides [31], the high-field signal at 1.9 ppm is caused by OH groups at the outer particle surface, while the signals at 6.8 and 11.5 ppm are low-field shifted due to internal interactions. Probably, the TiOH groups involved in these internal interactions are located in internal phase conjunctions visible in the TEM images of the sample TiO_2/A + R (see Figure 2b and d). The TiOH signals in the spectrum of TiO_2/A + R (Figure 4b) show a strong broadening probably due to a distribution of chemical shift caused by the low-ordered TiO_2 and internal interactions. The evaluation of the ^{1}H MAS NMR spectra in Figure 4 gave the TiOH densities summarized in Table 3. According to these values, the transformation of the pure-anatase TiO_2/A to the mixed-phase TiO_2/A + R is accompanied by a small decrease of the TiOH density and a slight change of the resonance position of the TiOH groups involved in internal interactions.

3.4. ^{17}O isotope exchange experiments on pure-anatase TiO_2/A and mixed-phase TiO_2/A + R

The OIE kinetics were investigated by recording the ^{17}O MAS NMR spectra of dehydrated TiO_2/A and TiO_2/A + R upon loading with 500 mbar $^{17}O_2$ gas and thermal treatment at 450, 500, and 550 °C for durations up to 100 h. As an example, Figure 5a and b show the stack plots of the ^{17}O MAS NMR spectra of TiO_2/A and TiO_2/A + R, respectively, recorded upon OIE at 500 °C. For TiO_2/A, the total intensity of the OTi_3 species at 562 ppm was evaluated to determine $^{16/17}O$ isotope exchange rates k (see, e.g., Figure 6) according to [32]:

$$I(t) = I(\infty)[1 - b \cdot \exp\{-k \cdot t\}] \quad (3)$$

where $I(t)$ and $I(\infty)$ denote the intensity of the ^{17}O MAS NMR signals the time t and in the equilibrium state, respectively, while the value b describes the exchange at $t = 0$. The obtained isotope exchange rates k are utilized for an Arrhenius plot allowing the determination of the OIE activation energy E_a via [14]:

$$k = A_0 \cdot \exp(-E_a/R \cdot T) \quad (4)$$

with the gas constant R, the isotope exchange temperature T, and the pre-exponential factor A_0.

The Arrhenius plot of the rates k obtained by evaluating the ^{17}O MAS NMR signal at 562 ppm in the spectra of pure-anatase TiO_2/A gives an activation energy of $E_a = 105 \pm 10$ kJ/mol (Figure 7 and Table 4). The plots of the ^{17}O MAS NMR intensities of the anatase and rutile signals at 562 and 596 ppm, respectively, in the spectra of TiO_2/A + R are shown in Figure 6a–c, closed symbols. Interestingly, activation energies of $E_a = 61 \pm 10$ kJ/mol and 70 ± 10 kJ/mol (Table 4) were obtained for the OIE with the anatase and rutile domains of TiO_2/A + R. For comparison, activation energies of

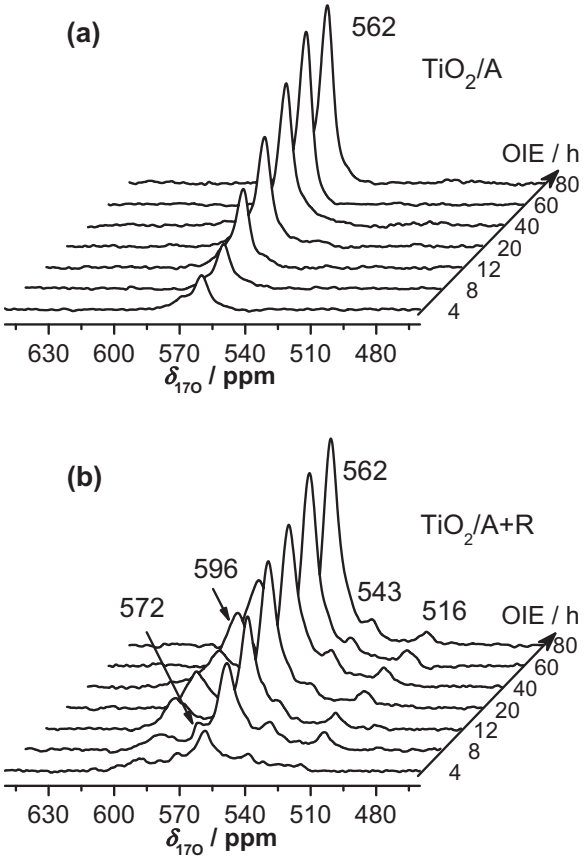

Figure 5. Stack plots of the ^{17}O MAS NMR spectra of TiO_2/A (a) and TiO_2/A + R (b) recorded after $^{16/17}O$ isotope exchange (OIE) at 500 °C for 4–80 h.

E_a = 134 and 144 kJ/mol were determined by Winter and Sturge [14] for the oxygen isotope exchange on pure-anatase and pure-rutile TiO_2, respectively, and of E_a = 105 kJ/mol for pure-anatase TiO_2/A in the present work. Hence, the activation energies for the OIE with anatase as well as rutile domains in the mixed-phase TiO_2/A + R are decreased by ca. 30% in comparison with that of the corresponding pure-phase materials.

Based on Pichat et al. [18], the above-mentioned strong decrease of the activation energy for the $^{16/17}O$ isotope exchange could be explained by the lability of surface oxygen atoms formed by the transformation of pure-anatase TiO_2/A into the mixed-phase TiO_2/A + R material. As demonstrated by the occurrence of ^{17}O MAS NMR signals at 516, 543, and 572 ppm in Figure 3b, surface oxygen species have a significant higher densities in mixed-phase TiO_2/A + R in comparison with pure-phase TiO_2/A.

In Figure 6a–c, open symbols, the intensities of the ^{17}O MAS NMR signals are plotted as a function of the oxygen isotope exchange time. Due to their much lower intensities in comparison with the ^{17}O MAS NMR signals of oxygen atoms in the anatase and rutile domains, no evaluation of the exchange kinetics for the surface oxygen sites is possible. However, an important characteristic of the ^{17}O MAS NMR signals at 516, 543, and 572 ppm is their very rapid increase, i.e. these signals increase in a much shorter time due to the $^{16/17}O$ isotope exchange compared with the anatase (562 ppm) and rutile (596 ppm) signals of the mixed-phase TiO_2/A + R. This observation indicates that the OIE in mixed-phase TiO_2/A + R starts at surface oxygen sites causing the ^{17}O MAS NMR signals at 516, 543, and 572 ppm. These surface oxygen species, on the other hand, cover the anatase and rutile domains or contribute to phase junctions between anatase and rutile domains. Therefore, a subsequent OIE between ^{17}O-enriched

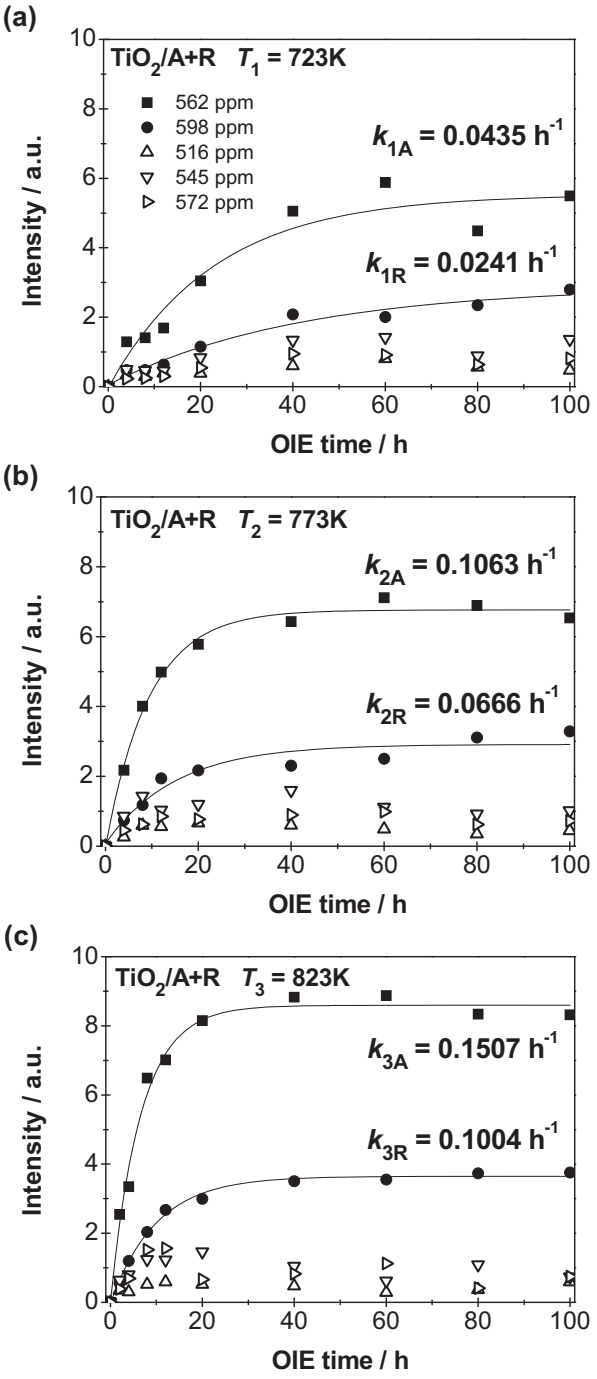

Figure 6. ^{17}O MAS NMR signal intensities of TiO_2/A + R at 516 ppm (distorted OTi_3 oxygen), 543 ppm (surface oxygen), 562 ppm (anatase), 572 ppm (oxygen in amorphous phases), and 596 ppm (rutile) plotted as a function of the $^{16/17}O$ isotope exchange (OIE) time for the exchange temperatures of 450 °C (a), 500 °C (b), and 550 °C (c).

surface oxygen species and ^{16}O atoms in the anatase and rutile domains occurs. The OIE via surface oxygen species in low-order TiO_2 layers may be the reason for the significantly lower activation energy of the OIE with anatase and rutile domains of TiO_2/A + R compared with that on pure-phase TiO_2/A materials characterized by a negligible low number of surface oxygen species.

According to the evaluation of the X-ray pattern of TiO_2/A + R (see Figure 1c), the anatase and rutile domains in this material have a ratio of ca. 1:1. However, a much lower relative intensity

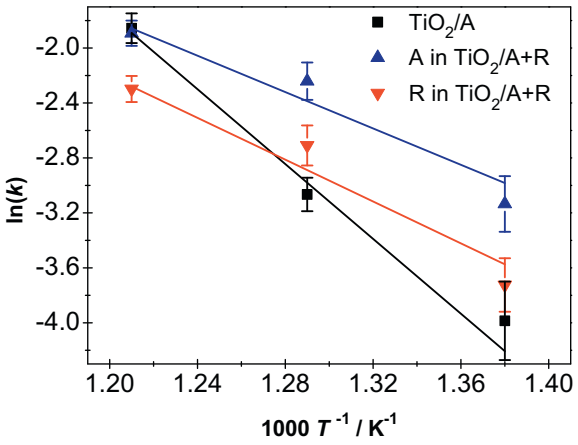

Figure 7. Arrhenius plots of the velocity constants k_i for the $^{16/17}O$ isotope exchange of oxygen atoms in the pure-anatase TiO_2/A (■) and in anatase (▲) and rutile domains (▼) of the mixed-phase TiO_2/A + R.

Table 4
Activation energies E_a of the $^{16/17}O$ isotope exchange of lattice oxygen atoms in the TiO_2 materials under study.

Sample	TiO_2 phase	E_a (kJ/mol)
TiO_2/A	Anatase	105 ± 10
TiO_2/A + R	Anatase	61 ± 10
TiO_2/A + R	Rutile	70 ± 10

of the ^{17}O MAS NMR signal of oxygen atoms in the rutile domains (596 ppm) in comparison with those in anatase domains (562 ppm) in TiO_2/A + R was found in the equilibrium state, as indicated by the curves in Figure 6 and the corresponding OTi_3 densities summarized in Table 3. Assuming that the $^{16/17}O$ isotope exchange occurs via surface oxygen species, which are responsible for the significant decrease of the activation energy of this exchange reaction, a higher content of rutile domains compared to anatase domains in the mixed-phase TiO_2/A + R must be formed inside the TiO_2 particles without having contact with surface oxygen species performing and accelerating the $^{16/17}O$ isotope exchange.

4. Conclusions

In this work, first quantitative ^{17}O MAS NMR investigation of the $^{16/17}O$ isotope exchange of oxygen atoms in the framework of pure-anatase and mixed-phase TiO_2 has been performed. For this purpose, a pure-anatase TiO_2/A material was synthesized via hydrolysis of $TiCl_4$, which was subsequently calcined to obtain a mixed-phase TiO_2/A + R material with anatase and rutile domains in the ratio of ca. 1:1 as determined by XRD. TEM images of TiO_2/A and TiO_2/A + R indicate that especially the latter material is covered by low-ordered TiO_2. On the other hand, a slightly lower TiOH density was found by ^1H MAS NMR spectroscopy for mixed-phase TiO_2/A + R compared with pure-phase TiO_2/A.

In the ^{17}O MAS NMR spectra of the mixed-phase TiO_2/A + R material, signals of OTi_3 oxygen species in anatase and rutile domains at 562 and 596 ppm, respectively, and of surface oxygen species at 516, 543, and 596 ppm were observed. In contrast, the spectrum of the pure-anatase TiO_2/A consists of a single signal at 562 ppm only, which is due to OTi_3 oxygen species of anatase. Interestingly, no ^{17}O MAS NMR signals were found in the spectral range described in literature for TiOH groups (−200 to 400 ppm). Hence, TiOH groups are not involved in the $^{16/17}O$ isotope exchange of dehydrated TiO_2 with $^{17}O_2$ gas. On the other hand, a significantly higher density of surface oxygen species in the mixed-phase TiO_2/A + R material compared to the pure-anatase TiO_2/A was found by ^{17}O MAS NMR spectroscopy.

As the most important result of the $^{16/17}O$ isotope exchange studies, a strong decrease of the activation energy of this exchange reaction on the mixed-phase TiO_2/A + R material (E_a = 61 (A) and 70 kJ/mol (R)) compared with the pure-anatase TiO_2/A (E_a = 105 kJ/mol) was determined. Furthermore, the very rapid increase of the ^{17}O MAS NMR signals of surface oxygen species in the TiO_2/A + R material indicates that the $^{16/17}O$ exchange reaction starts at these surface sites, which subsequently exchange with ^{16}O framework atoms in the anatase and rutile domains. By this way, the presence of a large density of surface oxygen species accelerates the $^{16/17}O$ isotope exchange in mixed-phase TiO_2. The much weaker content of ^{17}O-exchanged framework atoms in rutile domains compared with those in anatase domains of the mixed-phase TiO_2/A + R is explained by the formation of a significant content of rutile domains inside the mixed-phase TiO_2/A + R particles having no contact to surface oxygen species.

Acknowledgments

This work was supported by the Collaborative Innovation Center of Chemical Science and Engineering (Tianjin), 111 Project (B12015), MOE Innovation Team (IRT 13022), and the Ministry of Education of China (NCET-11-0251). Furthermore, M.H. wants to thank for financial support by Deutsche Forschungsgemeinschaft.

Appendix A. Supplementary data

Supplementary data associated with this article can be found, in the online version, at http://dx.doi.org/10.1016/j.cplett.2014.01.014.

References

[1] A. Fujishima, K. Honda, Nature 238 (1972) 37.
[2] M.R. Hoffmann, S.T. Martin, W.Y. Choi, D.W. Bahnemann, Chem. Rev. 95 (1995) 69.
[3] M.C.J. Bradford, M.A. Vannice, Appl. Catal. A 142 (1996) 73.
[4] G. Pfaff, P. Reynders, Chem. Rev. 99 (1999) 1963.
[5] A.L. Linsebigler, G.Q. Lu, J.T. Yates, Chem. Rev. 95 (1995) 735.
[6] T.L. Thompson, J.T. Yates, Chem. Rev. 106 (2006) 4428.
[7] U. Bach et al., Nature 395 (1998) 583.
[8] B. Oregan, M. Grätzel, Nature 353 (1991) 737.
[9] D.A.H. Hanaor, C.C. Sorrell, J. Mater. Sci. 46 (2011) 855.
[10] D.T. Cromer, K. Herrington, J. Am. Chem. Soc. 77 (1955) 4708.
[11] J. Zhang, Q. Xu, Z. Feng, M. Li, C. Li, Angew. Chem. Int. Ed. 47 (2008) 1766.
[12] J. Zhang, Q. Xu, M. Li, Z. Feng, C. Li, J. Phys. Chem. C 113 (2009) 1698.
[13] G.K. Boreskov, Adv. Catal. 15 (1965) 285.
[14] E.R.S. Winter, J. Chem. Soc. A (1968) 2889.
[15] J. Novakova, Catal. Rev. 4 (1971) 77.
[16] C. Doornkamp, M. Clement, V. Ponec, J. Catal. 182 (1999) 390.
[17] S. Sato, T. Kadowaki, K. Yamaguti, J. Phys. Chem. 88 (1984) 2930.
[18] P. Pichat, H. Courbon, R. Enriquez, T.T.Y. Tan, R. Amal, Res. Chem. Intermed. 33 (2007) 239.
[19] T.J. Bastow, A.F. Moodie, M.E. Smith, H.J. Whitfield, J. Mater. Chem. 3 (1993) 697.
[20] T.J. Bastow, G. Doran, H.J. Whitfield, Chem. Mater. 12 (2000) 436.
[21] E. Scolan, C. Magnenet, D. Massiot, C. Sanchez, J. Mater. Chem. 9 (1999) 2467.
[22] C.A. Klug, S. Kroeker, P.M. Aguiar, M. Zhou, D.F. Stec, I.E. Wachs, Chem. Mater. 21 (2009) 4127.
[23] D. Freude, in: R.A. Meyers (Ed.), Encyclopedia of Analytical Chemistry, Wiley, New York, 2000, p. 12188.
[24] M. Hunger, W. Wang, in: G. Ertl, H. Knoezinger, F. Schueth, J. Weitkamp (Eds.), Handbook of Heterogeneous Catalysis, vol. 2, Wiley-VCH, Weinheim, 2008, p. 912 (second ed., Chapter 3.1.3.7).
[25] K. Ding, Z. Miao, B. Hu, G. An, Z. Sun, B. Han, Z. Liu, Langmuir 26 (2010) 5129.
[26] M. Yan, F. Chen, J. Zhang, M. Anpo, J. Phys. Chem. B 109 (2005) 8673.
[27] R.A. Spurr, H. Myers, Anal. Chem. 29 (1957) 760.

[28] J. Yan, G. Wu, N. Guan, L. Li, Z. Li, X. Cao, Phys. Chem. Chem. Phys. 15 (2013) 10978.
[29] Y. Rao, T.F. Kemp, M. Trudeau, M.E. Smith, D.M. Antonelli, J. Am. Chem. Soc. 130 (2008) 15726.
[30] J. Blanchard, C. Bonhomme, J. Maquet, C. Sanchez, J. Mater. Chem. 8 (1998) 985.
[31] V.M. Mastkhin, I.L. Mudrakovsky, A.V. Nosov, Prog. NMR Spectrosc. 23 (1991) 259.
[32] H. Ernst, D. Freude, T. Mildner, H. Pfeifer, in: M.M.J. Treacy, B.K. Marcus, M.E. Bisher, J.B. Higgins (Eds.), Proceedings of the 12th International Zeolite Conference, Materials Research Society, Warrendale, USA, 1999, p. 2955.